Fizika Nizkikh Temperatur, 2003, v. 29, No. 2, p. 149–155

ab-plane tunneling and Andreev spectroscopy of superconducting gap and pseudogap in $(Bi,Pb)_2Sr_2Ca_2Cu_3O_{10+\delta}$ and $Bi_2Sr_2CaCu_2O_{8+\delta}$

A.I. D'yachenko[1], V.Yu. Tarenkov[1], R. Szymczak[2], H. Szymczak[2], A.V. Abal'oshev[2], S.J. Lewandowski[2], and L. Leonyuk[3]

[1]*A. Galkin Donetsk Physical and Technical Institute of the National Academy of Sciences of Ukraine 72 R. Luxemburg Str., Donetsk 83114, Ukraine*

[2]*Institute of Physics, Polish Academy of Sciences, 32/46 Al. Lotników, 02-668 Warsaw, Poland*
E-mail: abala@ifpan.edu.pl

[3]*Moscow State University, Moscow, 118899 Russia*

Received May 7, 2002, revised July 29, 2002

We have measured the temperature dependence of gap features revealed by Andreev reflection (Δ_s) and by tunneling (Δ) in the *ab*-plane of optimally and slightly overdoped microcrystals of $(BiPb)_2Sr_2Ca_2Cu_3O_{10+\delta}$ (Bi2223) with critical temperature T_c = 110–115 K, and $Bi_2Sr_2CaCu_2O_{8+\delta}$ (Bi2212) with T_c = 80–84 K. The tunneling conductance of a Bi2223 – insulator – Bi2223 junction shows peaks at the 2Δ gap voltage, as well as dips and broad humps at other voltages. In Bi2223, similarly to the well-known Bi2212 spectra, the energies corresponding to 2Δ, to the dip, and to the hump structure are in the ratio 2:3:4. This confirms that the dip and hump features are generic to the high-temperature superconductors, irrespective of the number of CuO_2 layers or the BiO superstructure. On the other hand, in both compounds the $\Delta(T)$ and $\Delta_s(T)$ dependences are completely different, and we conclude that the two entities are of different natures.

PACS: 74.25.Jb, **74.50.+r**, **74.72.–h**

1. Introduction

Along with the usual coherence gap Δ_s, in the spectrum of quasiparticle excitations in high-T_c superconductors there appears a gap Δ_p (pseudogap), which persists above the superconducting transition temperature T_c [1,2]. The pseudogap has the same *d* symmetry as Δ_s, but disappears (more accurately: becomes indistinct) at some temperature $T^* > T_c$ [3]. The relationship between the pseudogap and superconductivity is far from clear [1,2]. One of the reasons appears to be that the most popular methods of investigating the excitation spectrum in cuprates, like tunneling and angle-resolved photoemission (ARPES), cannot distinguish between Δ_p and Δ_s without recourse to various theoretical models. However, it is known that in the process of Andreev reflection of an electron from a normal metal–superconductor (N–S) interface, a Cooper pair is created in the superconductor [4]. This occurs only in the presence of a nonzero energy gap Δ_s in the superconductor. In other words, the process of Andreev transformation of an electron–hole pair into a Cooper pair is possible only for a reflection from the superconducting order parameter Δ_s. In marked contrast, the tunneling effect is sensitive to any singularity in the quasiparticle excitation spectrum [5]. Therefore, the tunneling characteristics at $T < T_c$ in general depend on joint contributions of the energy gap and pseudogap.

d-wave symmetry of the energy gap introduces some additional complications. The dominant contribution to the junction conductivity in classical (Giaever) tunneling comes from electrons with wave vectors forming a narrow, only a few degrees wide, cone [5]. Accordingly, tunnel junctions yield information on the gap anisotropy $\Delta(\mathbf{k})$, and the gap revealed in tunneling experiments can be expressed as $\Delta(\mathbf{k}) = [\Delta_s^2(\mathbf{k}) + \Delta_p^2(\mathbf{k})]^{1/2}$ [6]. In the case of Andreev reflection from a clean N–S interface, the situa-

tion is different. The incident electron is not scattered, but reflected back along the same trajectory. This is true for any angle of incidence. It can be said that all incident electrons participate in Andreev reflection on an equal footing. Therefore, measurement of a single Andreev N–S junction is in principle sufficient to determine the maximal value of the superconducting gap $\Delta_s(\mathbf{k})$.

In this paper we employ the above discussed characteristic features of tunneling and Andreev spectroscopy to investigate the temperature dependence of the energy gaps Δ and Δ_s in $Bi_2Sr_2CaCu_2O_{8+\delta}$ (Bi2212) and $(Bi,Pb)_2Sr_2Ca_2Cu_3O_{10+\delta}$ [(BiPb)2223] cuprates. The well-studied Bi2212 has two CuO_2 layers per unit cell and strong incommensurate modulation in the BiO layer [7], which complicates the interpretation of tunneling and ARPES data. The substitution of Bi by Pb in the (BiPb)2223 compound completely erases the superstructure in the BiO layers.

Tunneling measurements were carried out on «break junctions» with the barrier surface practically normal to the crystallographic axes in the base *ab* plane of the material. In the *c* direction, the influence of the BiO layer on the tunneling spectra is much more pronounced. Andreev experiments were performed on S–N–S junctions. In both cases we retained only the samples showing pure tunneling or Andreev characteristics. The temperature dependences of the energy gaps obtained in the two types of experiments are completely different and attest to fundamental differences between the «superconducting» gap Δ_s and the *a*,*b*-axis quasiparticle gap Δ.

2. Sample preparation

The tunnel junctions were elaborated from Bi2223 and Bi2212 single crystals. Textured $(Bi_{1.6}Pb_{0.4})Sr_2Ca_2Cu_3O_{10+\delta}$ and $Bi_2Sr_2CaCu_2O_8$ samples in the form of 10×1×0.1 mm rectangular bars were prepared [8–10] by compacting powdered (BiPb)2223 and Bi2212 compounds, respectively, at 30–40 kbar between two steel anvils. The powder was contained between two thin copper wires, whose deformation provided uniform pressure distribution in sample volume. In this manner the powder was compacted into dense plane-parallel bars about 0.1 mm thick. The bars were then pre-annealed at T = 845°C for 16 h, compressed again, and finally annealed at T = 830°C for 14 h, producing a well-pronounced texture. Usually the Bi2212 samples were slightly overdoped and exhibited a critical temperature T_c = 80–84 K. The doping level of the oxygen content was controlled by annealing optimally doped samples in flowing gas adjusted for different partial pressures of oxygen. The samples emerging from this procedure were highly

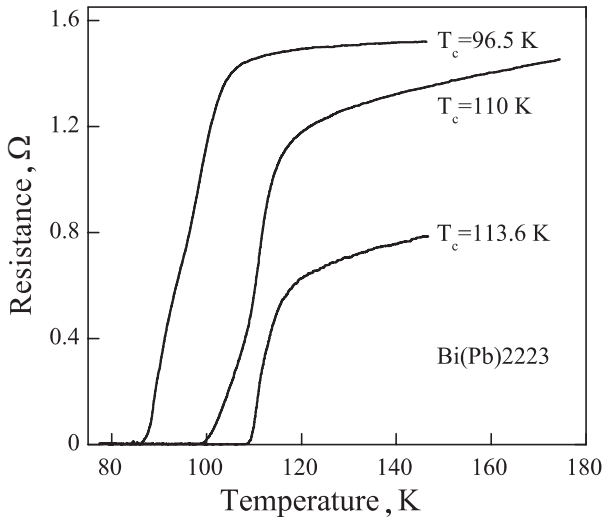

Fig. 1. Temperature dependence of the *ab*-plane resistance of (BiPb)2223 samples with different oxygen doping.

textured, composed of tightly packed microcrystals aligned in one direction. Sample quality was controlled by transport measurements. We used for further processing only those samples which were showing a critical current density J_c (T = 4.2 K) > $4{\cdot}10^4$ A/cm^2. The superconducting transition temperature T_c was determined from the midpoint of the resistive $R(T)$ transition (see Fig. 1).

The S–I–S and S–N–S junctions were made by breaking specially prepared Bi2212 and Bi2223 samples. Each sample was hermetically sealed by insulating resin and glued to an elastic steel plate, which was then bent until a crack occurred, running across the sample width and detected by monitoring the sample resistance. The hermetic seal remained unbroken in this process. After the external load was relieved, the sample returned to its initial position with the crack closed and the microcrystals once again tightly pressed to each other along the line of the fracture. The best alignment is expected in the sample region in which the shear deformation was minimal. This is apparently one of the reasons why such a procedure results in the realization of one effective junction of the microcrystal–microcrystal type. The selection of a single junction with minimal tunneling resistance from among the competing junctions is further assisted by the nature of the tunneling effect, which decreases exponentially with the barrier thickness. A small sample thickness (< 100 μm) and a relatively large size of the microcrystals (> 10 μm) are also important factors enhancing junction quality. Such break junctions on microcrystals were found to be particularly effective in the investigation of high-T_c superconductors [9]. The typical normal-state resistance of junctions used

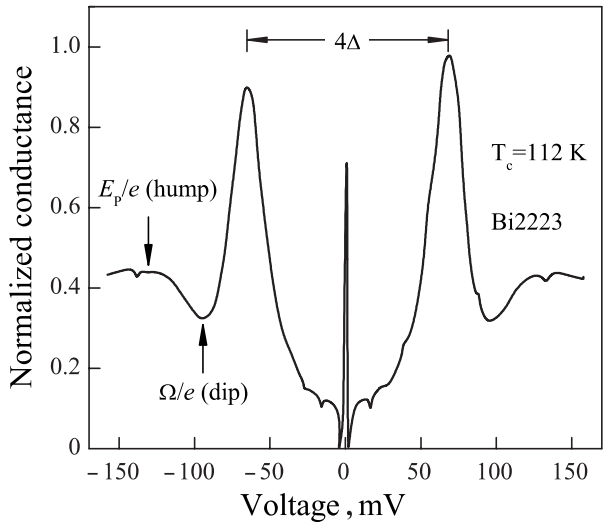

Fig. 2. Tunneling conductance of a Bi2223–I–Bi2223 junction at T = 77.4 K. The zero-bias peak is due to the Andreev bound state. The spectra clearly show dip and hump structures. Arrows indicate the 3Δ and 4Δ positions.

in the present study was between a few ohms and a few tens of ohms, and were remarkably stable.

The surface of our Bi2212 and (BiPb)2223 break junctions was perpendicular to the CuO_2 plane, and the direction of tunneling formed only a very small angle α with one of the crystallographic axes (*a* or *b*) in this plane, as is attested to by the presence of Andreev bound states, seen in the tunneling S–I–S characteristics as a characteristic peak of conductivity at zero bias (cf. Fig. 2). Numerical calculations based on a simplified theoretical model [9,11] and taking into account the *d*-wave mechanism of pairing show that the appearance of such a narrow zero-bias peak in the tunneling conductance occurs at $\alpha \leq 6°$. In high-quality break junctions the zero-bias conductance peak (ZBCP) was reported to coexist with the Josephson effect [12], but we have to rule out this possibility because of the wrong signature: the ZBCP was insensitive to magnetic field and did not reflect on the $I-V$ characteristics. The spectra $\sigma(V) = dI/dV$ show the quasiparticle peaks at 2Δ, where Δ is defined as a quarter of the peak-to-peak separation (Fig. 2). We use this Δ value as a measure of the gap, since there is no exact method of extracting the energy gap from the tunneling spectra, given that the exact functional form of the density of states for high-T_c superconductors is not known.

In general, the type of the junction was determined *ex post facto* from their conductance $\sigma(V)$ spectra. We retained for further investigation only the junctions conforming to either S–I–S or S–N–S types. For example, the $\sigma(V)$ curve in Fig. 2 reveals all the characteristic features of a superconducting tunnel S–I–S junction: an almost flat region around zero bias followed by a sharp increase in the tunneling current, peaking around ± 60 meV (2Δ); at still higher bias voltages V the conductance depends parabolically on V. The junction shown in Fig. 3, on the other hand, behaves as a typical Andreev S–N–S junction. First, there is a low-resistance region at low bias voltages, seen as a broad pedestal spanning the coordinate origin. The next indication is the excess current, which was observed in all S–N–S junctions included in this study. Finally, the differential conductivity of the junction at $eV > 2\Delta_s$ coincides with the normal-state conductivity at $T > T_c$ [see inset in Fig. 3,*b*], i.e., for $T > T_c$ practically all of the bias voltage is applied directly to the junction.

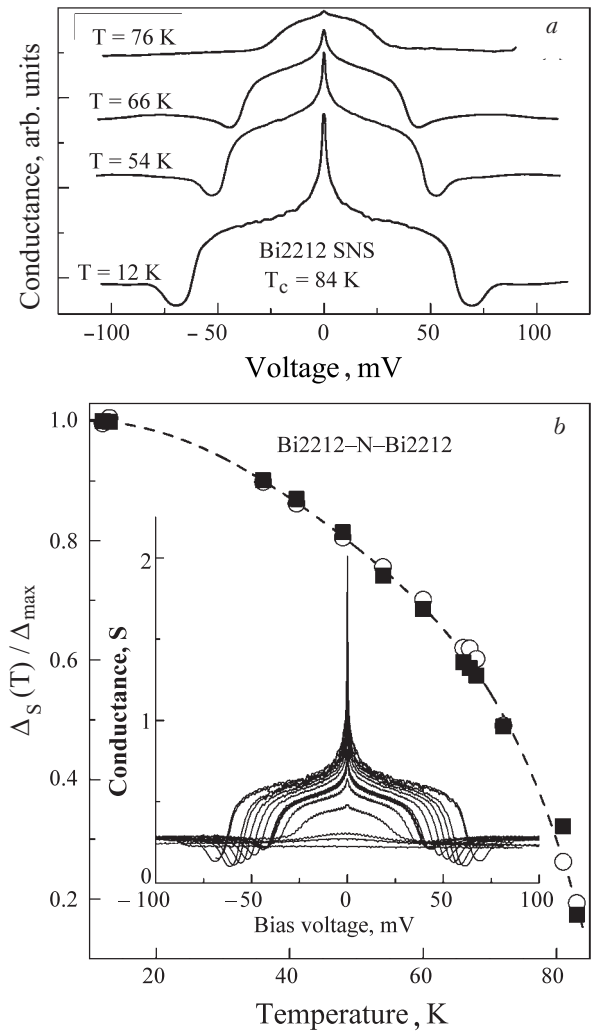

Fig. 3. Conductance σ of S–N–S (Andreev) Bi2212–N–Bi2212 break junction. (*a*) Temperature dependence of σ. The individual plots are shifted vertically for clarity. (*b*) Temperature dependence of the energy gap Δ_s. The inset shows the σ plots in their original position.

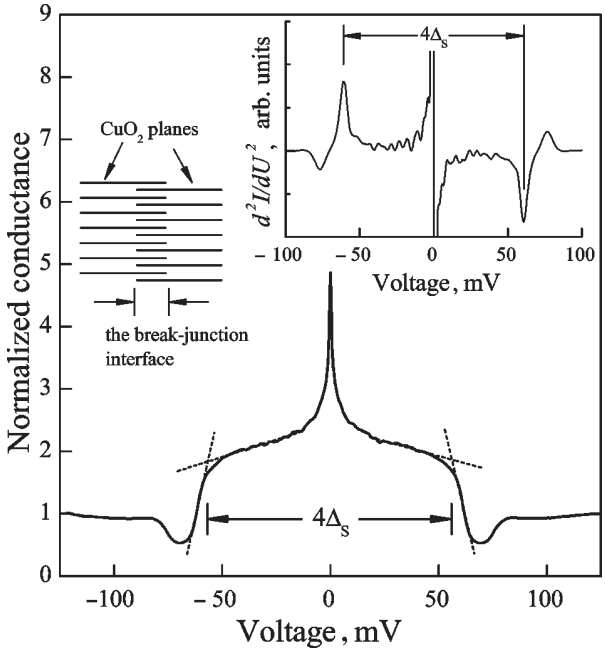

Fig. 4. Geometrical construction for the determination of Δ_s from Andreev measurements. The top inset shows the corresponding $d\sigma/dV$ plot. The left inset shows the hypothetical inner structure of the Andreev break junction.

One may inquire about the mechanism which might produce in an apparently random manner either S–I–S or S–N–S junctions. The insulating layer in S–I–S junctions is most probably caused by oxygen depletion. As to the normal barrier, we speculate that the CuO_2 planes are harder to fracture than the buffer layers. After the sample is broken, they penetrate slightly into the buffer layers (see left inset in Fig. 4). In this manner, the coupling between the CuO_2 planes belonging to the separated sample parts would be stronger than the normal coupling across the buffer layers, and it could assist in creating a constriction, which would act as a normal 3D metal. This hypothesis is in agreement with the scanning microscope study of the fracture surfaces of Bi2212 single-crystal break junctions, which revealed rough, but stratified fracture surfaces [13].

3. Experimental results

The temperature dependence of the energy gap $\Delta_s(T)$ obtained from Andreev S–N–S measurements for Bi2212 exhibited a BCS-like form (see Fig. 3). We used two methods to determine Δ_s for Andreev junctions. The first one is shown in Fig. 4 and relies on measuring the distance between the points of maximal slope changes of the $\sigma(V)$ plot, which is taken as the measure of $4\Delta_s$. The details of the second one are shown in top inset in Fig. 4. The rationale for both methods is in recent calculations [14], based on the

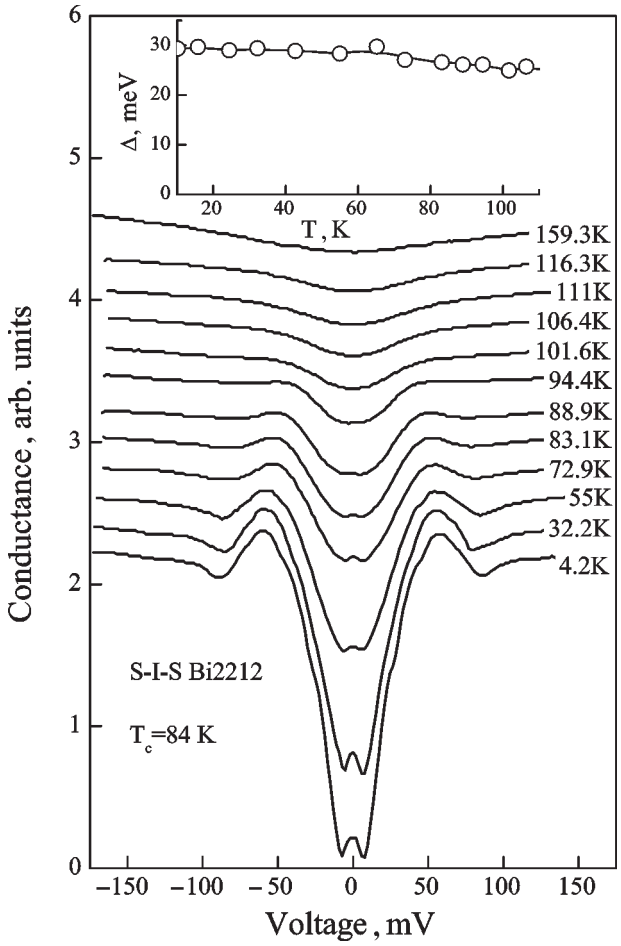

Fig. 5. Conductance of S–I–S (tunneling) Bi2223–I–Bi2223 break junction. The inset shows the temperature dependence of the tunneling gap $\Delta(T)$. Some structural details of the spectra have been blurred by the speed of recording needed to overcome temperature instabilities of the experimental setup.

Klapwijk, Blonder, and Tinkham [15] treatment of multiple Andreev reflections between two superconductors, which indicate that $2\Delta_s$ is determined by the separation of the extrema in $d\sigma/dV$. The results obtained by both methods are plotted together in Fig. 3,*b*. It is seen that these results differ slightly, but both outline essentially the same $\Delta_s(T)$ dependence.

The $\Delta(T)$ gap dependence determined from tunneling measurements performed on the same compounds diverged considerably from the BCS relation (Fig. 5). In fact, $\Delta(T)$ depends on temperature very weakly for $T \geq T_c$. According to an ARPES investigation [16], such behavior of $\Delta(T)$ in Bi2212 near optimal doping is expected for the *a* (or *b*) direction in the CuO_2 plane. This result agrees with our assumption about the direction of tunneling in our Bi2212–I–Bi2212 junctions. As mentioned above, further confirmation is provided by the presence of an Andreev bound state,

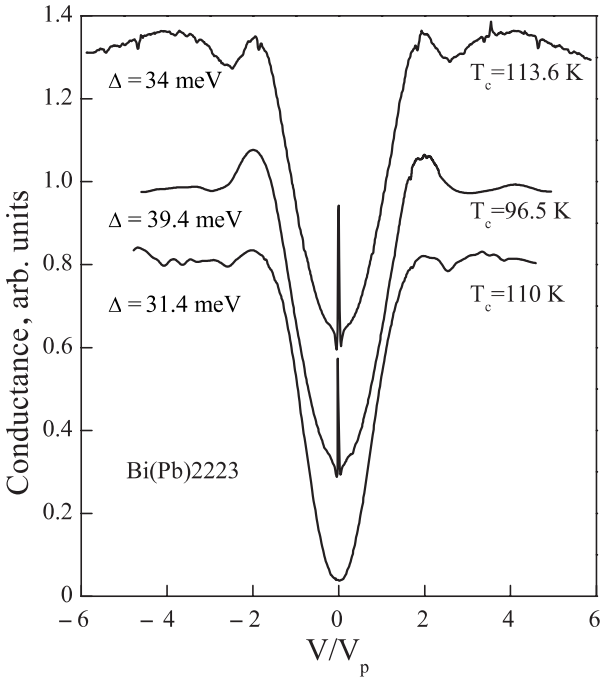

Fig. 6. S–I–S tunneling conductance in the *ab* plane for the Bi2223 samples of Fig. 1 at T = 77.4 K. The voltage axis has been rescaled in units of Δ. Each curve has been rescaled and shifted for clarity.

seen in the spectra of S–N–S and S–I–S junctions as a characteristic peak of conductivity at zero bias (cf. Fig. 3 and Fig. 5). According to the ARPES data [16], near optimal doping the $\Delta(T)$ gap becomes temperature dependent only when α is of the order of 15°. For technological reasons, the formation of break junctions with the crystal broken at such an angle is improbable. As a result, the tunneling characteristics at $T > T_c$ relate to the gap in (100) or (010) direction.

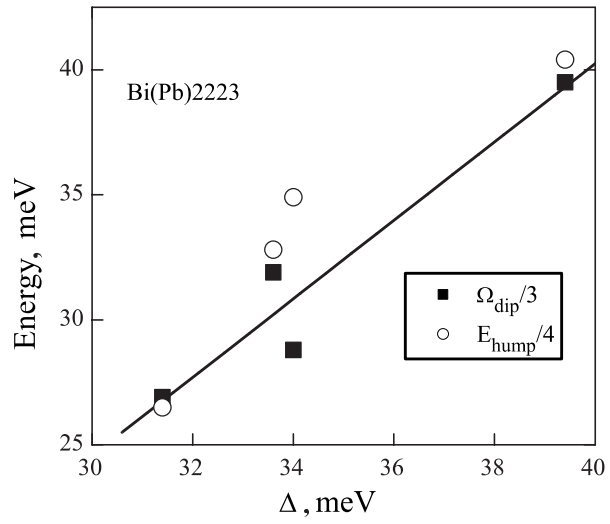

Fig. 7. Ω (dip) and E_p (hump) positions as a function of energy gap Δ, determined from the tunneling data of Figs. 2 and 6.

In full agreement with the ARPES results [16], with increasing temperature the gap Δ of Bi2212 becomes filled with quasiparticle excitations, and the conductance peaks at 2Δ become less distinct. The distance between the still-discernible conductance peaks does not decrease, and the $\Delta(T)$ gap is seen to persist into the region $T > T_c$. Similar behavior is also observed for the (BiPb)2223 compound.

The temperature dependence of the proper coherent gap $\Delta_s(T)$ behaves in a completely different manner (Fig. 3). The gap narrows with increasing temperature and at $T = T_c$ it closes completely. The high curvature of the Andreev conductance dip at $eV \approx 2\Delta_s$ is evidence both of the good quality of the investigated junctions and of the long lifetime of quasiparticles in the gap region. This was confirmed by the analysis of spectra of the normal metal–constriction–superconductor (N–c–S) junctions [9]. For Bi2212 Andreev N–c–S junctions, the Blonder – Tinkham – Klapwijk [17] parameter Z used to obtain the theoretical fit was small, $Z \simeq 0.5$, a value characteristic for very clean N–S contacts.

For energies beyond the gap Δ value, tunneling in the *ab* plane of (BiPb)2223 S–I–S junction revealed the so-called dip and hump structures, as shown in Fig. 2 and Fig. 6. In Fig. 6, the voltage axis is normalized to the voltage $eV_p = \Delta$, and the conductance axis is normalized to the background; the spectra are shifted vertically for clarity. The dip and hump features roughly scale with the gap Δ for different oxygen doping levels (see Fig. 7). There is, however, a slight deviation of the data from a straight line.

4. Theoretical implications

The considerable interest in pseudogap investigation is stimulated to a great extent by the theoretical models of high-T_c superconductivity, in which a pseudogap appears as a precursor of the superconducting gap [18,19], e.g., the bipolaron model [20]. In another group of models, the appearance of pseudogap is related to some sort of magnetic pairing [21]. However, the domains of applicability of these models are not very strictly defined and it is quite possible that the pseudogap (like high-temperature superconductivity) is caused by several simultaneously acting mechanisms.

For example, in the Emerson – Kilverson – Zachar (EKZ) theory [19] the crucial role in the formation of high temperature superconductivity is ascribed to the separation of spin and charge, arising as a result of partitioning of the CuO_2 planes into narrow conducting and dielectric stripes. «Pairing» at $T^* > T_c$ in the EKZ model means the formation of a spin gap. A wide

spin gap (or pseudogap Δ_p) is indeed formed in a spatially limited hole-free region, such as the region between the conducting stripes. A phase-coherent (i.e., actually superconducting) state is created only at $T < T_c$. The model explains well the smooth transition of the pseudogap into the tunneling gap Δ when the temperature decreases below T_c. However, the observed temperature dependence of the order parameter gap $\Delta(T)$ at $T < T_c$ is fundamentally different from that of the gap $\Delta_s(T)$, as is seen in Figs. 3 and 5. It is not clear how the BCS-like $\Delta_s(T)$ dependence arises in the phase-fluctuation picture. Such a situation would be possible, e.g., in the generation of charge (and spin) density waves, with the superconducting gap and pseudogap competing for the same region of the Brillouin zone [22]. Then the transition to the superconducting state could occur in the presence of a pseudogap in normal excitations, opening, e.g,. in the electron–hole channel (i.e., a pseudogap, which would not transform directly into the superconducting gap, as in the Emery–Kivelson model).

There are numerous experiments that confirm the essentially different nature of the superconducting gap Δ_s and the gap (pseudogap) Δ [23–25]. The most convincing are intrinsic *c*-axis tunneling experiments (in stacked layers) [26]. However, they yield different results from the point contact, scanning tunneling spectroscopy (STM), and break junction experiments: the hump was observed at an energy of 2Δ instead of 4Δ. The authors note a similarity between the observed *c*-axis pseudogap and Coulomb pseudogap for tunneling into a two-dimensional electron system. In our case, the tunneling and Andreev reflection were realized in the *ab* plane, and together with the $\Delta(T)$ dependence (Fig. 4), we clearly observed the peak–dip–hump structure (Figs. 2 and 3). The position of the dip and hump for S–I–S junctions was at 3Δ and 4Δ (Fig. 2). This suggests that the observed dip–hump structure may originate from short-range magnetic correlations in the *ab* plane [27]. Then the gap Δ would be the fermionic excitation gap and Δ_s – the mean-field order parameter. It should be emphasized, finally, that the observed $\Delta_s(T)$ dependence exhibits non-BCS behavior at $T \to 0$ (Fig. 3).

In summary, our *ab*-plane tunneling and Andreev spectroscopy studies of normal and slightly overdoped (BiPb)2223 and Bi2212 compounds show the presence of both a superconducting energy gap Δ_s, corresponding to *d*-wave Cooper pairing, and a dip–hump structure at 3Δ and 4Δ (for the S–I–S junction). This suggests that the high-energy pseudogap, which is associated with the dip and hump, could be magnetic in origin. The gap Δ is nearly temperature independent and becomes blurred above T_c, being continuously transformed with increasing temperature into the pseudogap. In contrast, the order parameter gap $\Delta_s(T)$ has a strong temperature dependence and for $T \to 0$ reveals a non-BCS mean field behavior. Our findings are in general agreement with those of Deutscher [25], although it must be emphasized again that we have considered the slightly overdoped case.

Acknowledgments

This work was supported by Polish Government (KBN) Grant No PBZ-KBN-013/T08/19.

1. T. Timusk and B. Statt, *Rep. Prog. Phys.* **62**, 61 (1999).
2. T. Tohoyama and S. Maekawa, *Supercond. Sci. Technol.* **13**, R17 (2000).
3. Ch. Renner, B. Revaz, J.-Y. Genoud, K. Kadowaki, and Ø. Fischer, *Phys. Rev. Lett.* **80**, 149 (1998).
4. A.F. Andreev, *Sov. Phys. JETP* **19**, 1228 (1964).
5. E.L. Wolf, *Principles of Electron Tunneling Spectroscopy*, Oxford University Press, New York (1985).
6. J.L. Tallon and G.V.M. Williams, *Phys. Rev. Lett.* **82**, 3725 (1999).
7. M.A. Subramanian, C.C. Torardi, J.C. Calabrese, J. Gopalakrishnan, K.J. Morrissey, T.R. Askew, R.B. Flippen, U. Chowdhry, and A.W. Sleight, *Science* **239**, 1015 (1988).
8. A.I. Akimenko, T. Kita, J. Yamasaki, and V.A. Gudimenko, *J. Low. Temp. Phys.* **107**, 511 (1997).
9. A.I. D'yachenko, V.Yu. Tarenkov, R. Szymczak, A.V. Abal'oshev, I.S. Abal'osheva, S.J. Lewandowski, and L. Leonyuk, *Phys. Rev.* **B61**, 1500 (2000).
10. V.M. Svistunov, V.Yu. Tarenkov, A.I. Dyachenko, and R. Aoki, *Physica* **C314**, 205 (1999).
11. Y. Tanaka and S. Kashiwaya, *Phys. Rev. Lett.* **74**, 3451 (1995).
12. A.M. Cucolo, A.I. Akimenko, F. Bobba, and F. Giubileo, *Physica* **C341-348**, 1589 (2000).
13. A.I. Akimenko, R. Aoki, H. Murakami, and V.A. Gudimenko, *Physica* **C319**, 59 (1999).
14. A.I. D'yachenko, *private communication* (2002).
15. T.M. Klapwijk, G.E. Blonder, and M. Tinkham, *Physica* **B109–110**, 1657 (1982).
16. M.R. Norman, H. Ding, M. Randeria, J.C. Campuzano, T. Yokoya, T. Takeuchi, T. Takahashi, T. Mochiku, K. Kadowaki, P. Guptasarma, and D.G. Hinks, *Nature* **392**, 157 (1998).
17. G.E. Blonder, M. Tinkham, and T.M. Klapwijk, *Phys. Rev.* **B25**, 4515 (1982).
18. V.J. Emery and S.A. Kivelson, *Phys. Rev. Lett.* **74**, 3253 (1995); *Nature* **374**, 434 (1995).
19. V.J. Emery, S.A. Kivelson, and O. Zachar, *Phys. Rev.* **B56**, 6120 (1997).
20. A.S. Alexandrov, *Philos. Trans. R. Soc. London* **A356**, 197 (1998) (and references therein).

21. P.W. Anderson, *The Theory of Superconductivity in the High-T_c Cuprate Superconductors*, Princeton University Press, Princeton (1997).
22. R.S. Markiewicz, C. Kusko, and V. Kidambi, *Phys. Rev*. **B60**, 627 (1999).
23. Q. Chen, K. Levin, and I. Kosztin, *Phys. Rev*. **B63**, 184519 (2001).
24. V.V. Kabanov, J. Demsar, B. Podobnik, and D. Mihailovic, *Phys. Rev*. **B59**, 1497 (1999).
25. G. Deutscher, *Nature* **397**, 410 (1999).
26. V.M. Krasnov, A. Yurgens, D. Winkler, P. Delsing, and T. Claeson, *Phys. Rev. Lett*. **84**, 5860 (2000).
27. N. Miyakawa, J.F. Zasadzinski, L. Ozyuzer, P. Guptasarma, D.G. Hinks, C. Kendziora, and K.E. Gray, *Phys. Rev. Lett*. **83**, 1018 (1999).